Journal of King Saud University – Science 34 (2022) 101925

Contents lists available at ScienceDirect

Journal of King Saud University – Science

journal homepage: www.sciencedirect.com

Original article

# Rejection of the internal α background in $LaBr_3$:(Ce) detectors by using a wavelet-based pulse-shape discrimination method

Thamer Alharbi

*Department of Physics, College of Science in Zulfi, Majmaah University, Majmaah 11932, Saudi Arabia*

ARTICLE INFO

*Article history:*
Received 19 November 2021
Revised 7 February 2022
Accepted 22 February 2022
Available online 26 February 2022

*Keywords:*
$LaBr_3$:(Ce)
Pulse-shape discrimination
γ-Ray spectroscopy
Internal radiation

ABSTRACT

$LaBr_3$:(Ce) exhibits the best energy resolution among scintillation γ-ray detectors. The excellent energy resolution of this detector has made it suitable for many radiation detection applications such as environmental monitoring, medical imaging, nuclear security, nuclear physics experiments, etc. However, $LaBr_3$:(Ce) crystal endures from internal radioactivity which produces a considerable background in the measurements. The problem of internal radiation is particularly acute with large size detectors, measuring low-intensity γ-rays. A considerable part of the internal radiation comes from the α-decay of $^{227}$Ac and its daughters which are present as an impurity in the detector's crystal. Unfortunately, due to the very similar chemical properties of Actinium and Lanthanum, it is very difficult to remove the $^{227}$Ac impurity by using purification processes, and therefore, the α-background is present in all the commercial crystals. A practical approach for the reduction of this problem is to identify the α-events through an electronic analysis of the shape of output pulses of the detector and reject them. In the past, several digital pulse-shape discrimination (PSD) methods have been proposed to suppress the internal α background in $LaBr_3$:(Ce) detectors. These methods exploit the small difference in the shape of scintillation pulses from α- and γ-ray interactions. The PSD methods have demonstrated some degree of success, which are limited to only a partial rejection of the α-background while further reduction of the α background is highly desirable for low-background γ-ray measurements. In this work, a novel digital PSD method that significantly improves the rejection of the internal α background was developed. The PSD method is based on the wavelet transform of the scintillation pulses, leading to an almost complete rejection of the α background. This method is very useful for low-level radiation measurements with $LaBr_3$:(Ce) detectors involving high-energy γ rays.



## 1. Introduction

The cerium-doped lanthanum tribromide ($LaBr_3$:(Ce)) crystal is a well-established high-energy-resolution γ-ray scintillation detector (van Loef et al., 2001; Alharbi et al., 2015). Owing to the high yield of the scintillation light (~65 photons/keV), an energy resolution of ~3% (FWHM) at an energy of 662 keV can be achieved with this scintillator, which is the best energy resolution among those of the known scintillators (van Loef et al., 2002). In addition, the very fast decay time constant of ~15 ns makes this detector suitable for fast timing measurements (Alharbi et al., 2015; Vedia et al., 2017). Moreover, $LaBr_3$:(Ce) crystals have a high detection efficiency and are relatively stable against temperature variations. The effect of temperature on the light yield and decay-time constant of $LaBr_3$:(Ce) crystals was investigated by Moszyński et al. (2006) and Bizarri et al. (2006), who demonstrated that the effect is relatively small. However, this scintillator suffers from internal radiation, part of which is due to α emissions with energies of >1.5 MeV from progenies of $^{227}$Ac contamination in the detector's crystal (Wolszczak and Dorenbos, 2017; Nicolini et al., 2007). The half-life of $^{227}$Ac is 21.7 years and its decay generates a cascade of daughters, each with a different half-life. The contribution of the α emissions from $^{227}$Ac and its daughters was evaluated to be ~12% of the total internal background of $LaBr_3$:(Ce) crystals. The rest of the background contains γ-rays, beta-rays, and x-rays which result from the decay chain of $^{138}$La. The α background limits the measurement of weak intensity γ rays in the high-energy region; for this reason, the electronic discrimination of α-particle

E-mail address: t.alharbi@mu.edu.sa
Peer review under responsibility of King Saud University.

Production and hosting by Elsevier

https://doi.org/10.1016/j.jksus.2022.101925

and $\gamma$-ray events can be very useful for low-background measurements involving high-energy $\gamma$-rays. Several digital pulse-shape discrimination (PSD) techniques with different degrees of success have been proposed for this purpose (Hoel et al., 2005; Crespi et al., 2009; Ogawara and Ishikawa, 2015; McFee et al., 2016; Alharbi, 2020, Zeng et al., 2016). In this study, a new digital PSD technique based on the wavelet transform of scintillation pulses is reported. This technique advances to a significant improvement in the rejection of the $\alpha$ background. The details of the method are described, and the excellent performance of the method for almost complete discrimination of $\alpha$ particles and $\gamma$ rays is experimentally demonstrated.

## 2. PSD in $LaBr_3$:(Ce) detectors

The difference in the shape of $\alpha$-particle and $\gamma$-ray output pulses from $LaBr_3$:(Ce) detectors has been previously characterized in various studies (Hoel et al., 2005; Crespi et al., 2009; Zeng et al., 2016; Cang et al., 2020). The difference in the shape of the pulses is due to the fact that in the lanthanum halide scintillators, the amplitude of the scintillation constituent with the fastest decay time constant is slightly suppressed with $dE/dx$ (Hoel et al., 2005; Cang et al., 2018, 2020). For $\alpha$-particle and $\gamma$-ray pulses of the same energy, the difference in the shape of the pulses appears at the leading edge of the pulses with a maximum difference around the peaks (Alharbi, 2020). The maximum difference between the pulses is on the order of 10% (Crespi et al., 2009). From a qualitative point of view, the leading edge of a signal generated by $\alpha$ particles is slightly faster than that generated by a $\gamma$ ray of the same energy. The PSD algorithms examined so far to exploit the differences in the shapes of $\alpha$-particle and $\gamma$-ray pulses from $LaBr_3$:(Ce) include the charge-comparison method (Crespi et al., 2009; Zeng et al., 2016), the peak-to-charge ratio method (Ogawara and Ishikawa, 2015), principal component analysis (Alharbi, 2020), $\gamma$–$\alpha$ model analysis (Zeng et al., 2016), and the mean time method (Zeng et al., 2016). However, all these methods have only achieved partial rejection of the $\alpha$ background.

## 3. Wavelet-based PSD method

The wavelet transform has already been used for the analysis of pulses from radiation detectors in several applications (e.g., Yousefi et al., 2009; Singh and Mehra, 2017). The wavelet transform allows one to simultaneously analyze the signals over both time and frequency, and thus it can provide more information about a signal than the common Fourier transform, where a signal is evaluated only in the frequency domain. The continuous wavelet transform $W_f$ of signal $f(t)$ at time $u$ and scale $s$ is defined as

$$W_f(u,s) = \int_{-\infty}^{+\infty} f(t)\frac{1}{\sqrt{s}}\varphi^*\left(\frac{t-u}{s}\right)dt, \quad (1)$$

where $t$ is the time, $s$ is the scaling factor, $\phi$ is called the mother wavelet, and the star indicates the complex conjugate. The mother wavelet is a source function for the generation of daughter wavelets, which are simply translated and scaled versions of the mother wavelet. The scale is used for the characterization of the frequency contents of the signal, while translation is used for the localization of different frequency contents. There are several choices available for the mother wavelet, and the best choice depends on the application. In general, the choice of wavelet depends on the feature of interest from within the signal. Because the difference between the $\alpha$-particle and $\gamma$-ray pulses lies in their rise time, our aim is to use a mother wavelet that is sensitive to the degree of sharpness in the leading edge of the pulses; for this reason, the Haar wavelet is a good choice (Tang, 2014). The Haar wavelet has been widely used for the detection of sharp transitions in one-dimensional signals and has the advantage of simple implementation. Because an $\alpha$ pulse has a sharper leading edge than a $\gamma$-ray pulse, the amplitude of the Haar wavelet transform of the $\alpha$ pulse should produce an output with a greater amplitude than that of a $\gamma$-ray pulse of the same energy. This property was used in a PSD approach that simply compares the amplitude of the Haar wavelet transform of a pulse against the energy of the pulse.

## 4. Experimental setup

The performance of the PSD method was examined by using a $LaBr_3$:(Ce) detector (AS20, BrilLanCe™ Saint Gobain) whose crystal has a cylindrical shape (2″ × 2″) and is coupled to a photomultiplier tube (R6231, Hamamatsu Photonics). The crystal contains five percent of cerium dopant. The photomultiplier tube was biased at 700 V. The output pulses from the anode of the photomultiplier tube were digitized and recorded using a fast digital oscilloscope with 8-bit resolution and 250-ps sampling intervals. Each pulse was recorded for 150 ns (600 samples). The waveforms were copied to a personal computer to be analyzed offline. The analysis of the signals was performed using the wavelet toolbox of the MATLAB package.

## 5. Results

Fig. 1 shows the results of the characterization of the detector with a $^{60}$Co $\gamma$-ray source. The $\gamma$-ray energy spectrum of $^{60}$Co was obtained by making a histogram of the total charge of the scintillation pulses. The total charge (energy) of each pulse was determined by taking a numerical integration of the pulse's samples. Prior to the numerical integration, the offset of each pulse was fixed by subtracting the average value of the first 80 samples of pulses before the oscilloscope's trigger level from the pulse. The two peaks at 1.17 MeV and 1.33 MeV were fitted with Gaussian functions and the energy resolutions were determined by dividing the Full-Width at Half-Maximum (FWHM) of the peaks to the corresponding energies. The energy spectrum exhibits energy resolutions of 2.89% (FWHM) and 2.56% (FWHM), respectively, at 1.17 and 1.33 MeV $\gamma$-ray peaks, which are consistent with the common values reported in the literature.

After the initial characterization of the system with a $^{60}$Co $\gamma$-ray source, 100,000 pulses were collected from the internal radiation of the detector. For this purpose, the measurement was taken in a low-activity room and under lead shielding, where ambient radiation was low in comparison to the internal radiation from the $LaBr_3$:(Ce) detector. To extract a discrimination factor for the discrimination between the $\alpha$ pulse and $\gamma$-ray pulses, the Haar wavelet transform of the pulses was calculated using the *CWT* function in the MATLAB package. This function calculates the wavelet transform of the input signal for a determined scale value. The amplitude of the wavelet transform of each pulse was then determined and normalized to the energy of the scintillation pulse to be used as a discrimination factor. Fig. 2 shows a scatter plot of the discrimination factor against the energy of the events. A scale value of 15 ns was used in the calculation of the Haar wavelet transform. In the energy range of 1500–3000 keV, the scatter plot features two well-defined regions, characteristic of well-separated $\alpha$ particles (upper) and $\gamma$ rays (lower). According to several studies (Milbrath et al., 2005; Dorenbos et al., 2004), the light yield of $\alpha$ particles in the $LaBr_3$:(Ce) crystal is considerably lower than that for $\gamma$ rays. Therefore, although the actual energy of the $\alpha$ particles emitted from $^{227}$Ac and its daughters are on the order of several MeV, the $\alpha$ pulses appear in the energy range of 1.5–3.0 MeV

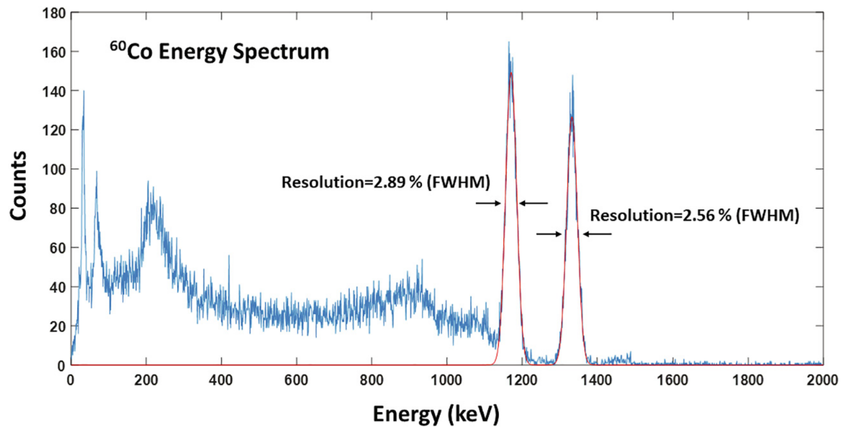


**Fig. 1.** Characterization of the γ-ray spectroscopic performance of the detector with digital processing of the photomultiplier's output pulses by using a $^{60}$Co γ-ray source. The energy resolutions are 2.89 and 2.56 % at, respectively, at 1.17 and 1.33 MeV energies. The low energy peaks are due to 32 keV x-rays and beta continuum from $^{138}$La, and backscattered γ-rays from $^{60}$Co source.

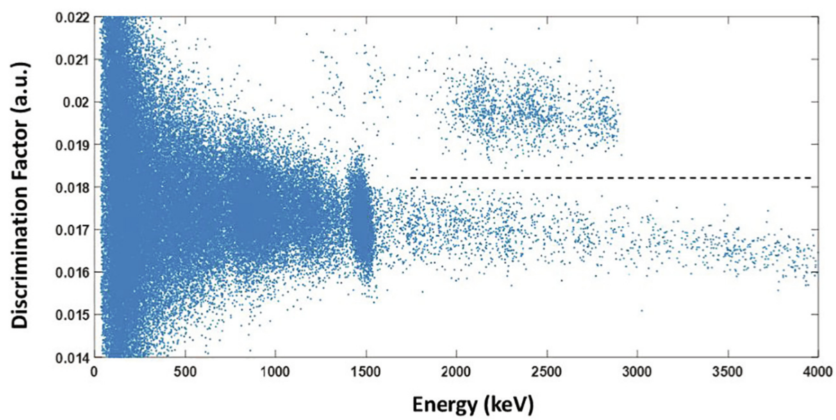


**Fig. 2.** Scatter plot of the discrimination factor against the event energy. The α particles and γ rays are well separated to different regions. The vents with a discrimination factor above 0.018 are α-particles and events with a discrimination factor below 0.018 are γ-rays. The scale factor in the wavelet transform is 15 ns.

and interfere with the γ-ray measurements in this energy range. Fig. 2 shows that the discrimination between the α-particle and γ-ray events in the wavelet method can be simply obtained by defining a boundary, and the events were classified as α particle if the discrimination factor was > 0.018 or γ ray if the discrimination factor was < 0.018. Fig. 3 shows the background spectrum after the rejection of α particle background events in the energy region above 1.5 MeV together with the spectrum of the rejected background α particle events. One can see that the α particles background consists of three wide peaks.

The performance of the PSD method may be quantitatively checked by calculating the figure of merit (FOM) for the

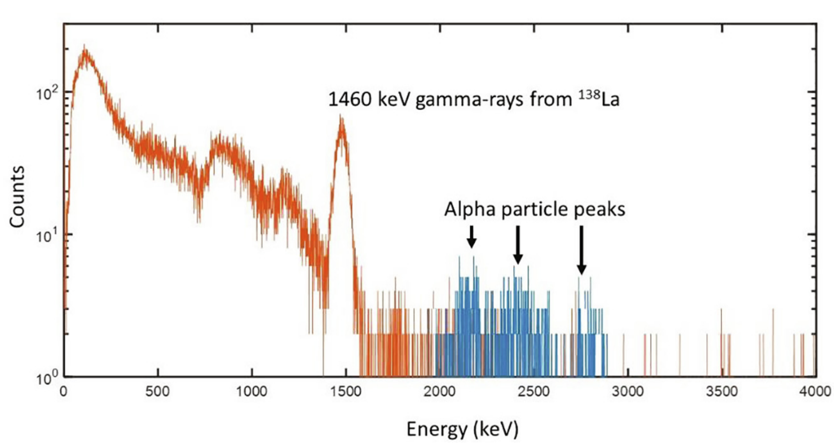


**Fig. 3.** The energy spectrum of background events after the rejection of α particles together with the spectrum of background α particles. One can see that the α particles events lie in three separate peaks corresponding to the energy of α particles from the decay of $^{227}$Ac and its daughters.

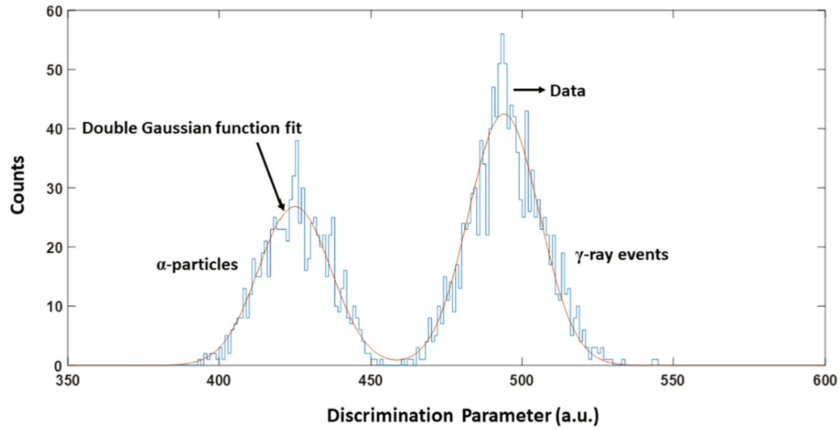


**Fig. 4.** Calculation of the FOM value for the wavelet PSD method with a scale value of 15 ns. A FOM value of 1.25 ± 0.05 was achieved.

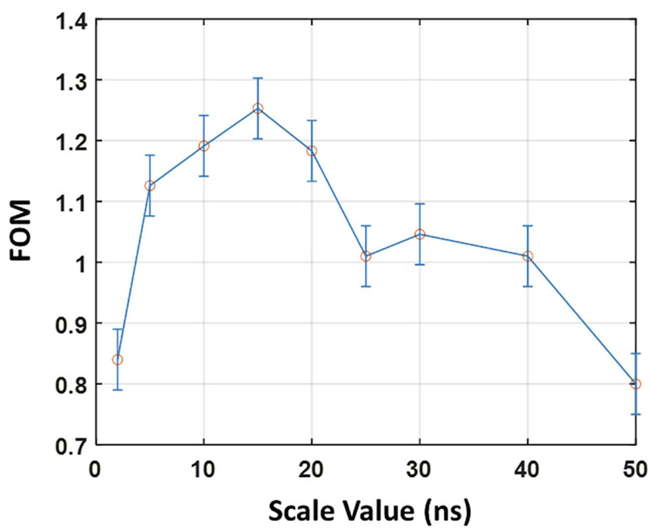


**Fig. 5.** Variation of the FOM value with the scale value in the Haar wavelet transform of the scintillation pulses.

distribution of the discrimination factor (R. A. Winyard, et al, 1971). The FOM is defined as

$$\text{FOM} = \frac{D}{\text{FWHM}_{\alpha} + \text{FWHM}_{\gamma}}, \tag{2}$$

where $D$ is the separation between the peaks of the α-particle and γ-ray events and $\text{FWHM}_{\alpha}$ and $\text{FWHM}_{\gamma}$ are the FWHM values of the distributions of α-particle and γ-ray peaks, respectively. These parameters are determined by fitting a double Gaussian function to the distribution of the discrimination factor. Fig. 4 shows the results of the FOM calculations corresponding to the data shown in Fig. 2. Both peaks of α-particle and γ-ray events exhibit good Gaussian shapes over the entire energy range of 1500–3000 keV. A very good FOM value of 1.25 ± 0.05 was obtained by fitting a double Gaussian function to the distribution. The error was calculated based on errors in the fitting process. Because the scale value in the wavelet transform strongly affects the result of the transform and, thereby, the PSD performance, the PSD method was repeated for a range of scale values, and the corresponding FOM values were calculated using Eq. (2). Fig. 5 shows the variations in the FOM value with the scale value. The optimum scale value was ~ 15 ns.

**Table 1**
Comparison of the FOM values of different digital PSD methods previously examined for the rejection of α background in $LaBr_3$:(Ce) detectors.

| Method | FOM | Reference |
|---|---|---|
| Principal component analysis | 0.92 | (Alharbi, 2020) |
| Charge comparison | 0.686 | (Zeng et al., 2016) |
| Mean time method | 0.503 | (Zeng et al., 2016) |
| Pulse model | 0.623 | (Zeng et al., 2016) |
| Wavelet transform | 1.25 ± 0.05 | Current work |

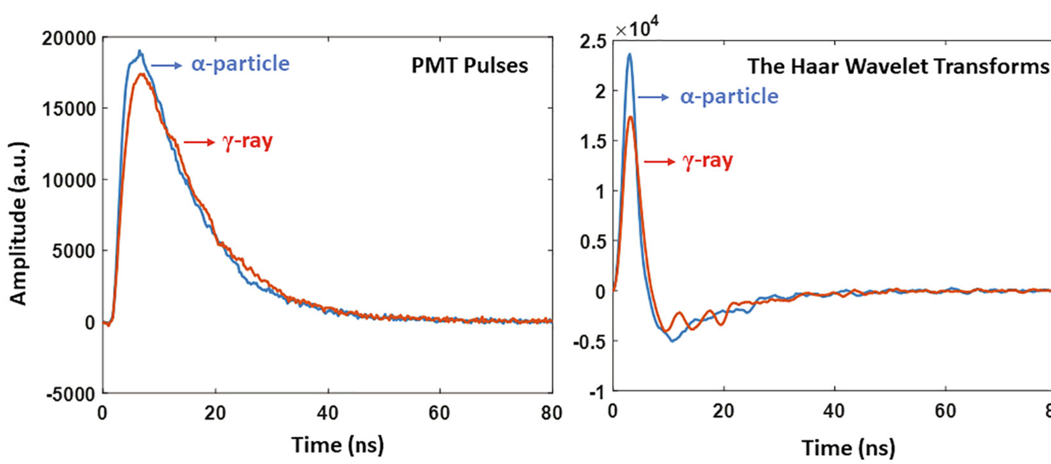


**Fig. 6.** Two example α-particle and γ-ray pulses, together with their corresponding Haar wavelet transforms with a scale value of 15 ns. Both pulses have the same energy. The ratio of the amplitude of the photomultiplier output pulses is only 1.05 while the ratio of the amplitude of the Harr wavelet transforms of the pulses is ~ 1.36.

Two typical α-particle and γ-ray pulses, together with their corresponding wavelet transforms obtained with a scale value of 15 ns, are shown in Fig. 6. The pulses were selected to have the same energy of ∼ 2 MeV. It is apparent that, while the amplitudes of the original scintillation pulses are only slightly different, the difference in the amplitude of the wavelet transforms of the pulses is ∼ 20%, which reflects the high sensitivity of the wavelet PSD method to the difference in the shape of the scintillation pulses.

## 6. Discussion

As already mentioned, digital PSD methods have been previously used to discriminate between α-particle and γ-ray pulses from $LaBr_3$:(Ce) detectors. However, owing to the small difference in the shape of the pulses, the previous PSD methods have been able to discriminate only against a fraction of the α-particle pulses. The reported FOM values for the previous PSD methods and the current work are summarized in Table 1. It can be seen that the wavelet-based PSD method exhibits the highest FOM value, which means that the wavelet method offers significantly improved performance over the previous PSD methods, and therefore, the overlap areas between the α-particle and γ-ray events have significantly decreased. In general, it has been shown that a complete separation of the two classes of events with Gaussian distributions is achieved when the FOM value exceeds a threshold level of 1.27 (Lintereur et al., 2002). Based on this baseline, our PSD method with an FOM value of 1.25 ± 0.05 can achieve almost complete rejection of the α-contamination background. It is worth mentioning that actinium has very similar chemical properties to lanthanum because its location in the periodic table is directly below lanthanum, which makes it a very difficult contaminant to eliminate. In fact, Ac contamination is still present in all the commercial $LaBr_3$:(Ce) crystals; therefore, our electronic elimination of background brings a significant advantage to $LaBr_3$:(Ce) without extra cost. The significant improvement in the performance of $LaBr_3$:(Ce) detectors enables the measurement of low-intensity energetic γ rays with this high-energy-resolution detector. There are many applications that can benefit from the elimination of α background in $LaBr_3$:(Ce) detectors, including gamma-scanning systems for identifying potential sources of contamination in the environment and soil, nuclear security systems for the detection of illegal nuclear materials, nuclear physics experiments, and radioisotope identification devices.

## 7. Conclusions

A new digital PSD method for the rejection of α background in $LaBr_3$:(Ce) detectors is developed. The method is based on the Haar wavelet transform of scintillation pulses, which is a simple and easy to implement method. The simplicity of the method makes it possible to implement it on digital hardware for real-time operations and build a digital γ-ray spectroscopy system. Evaluation of the method through the calculation of the FOM demonstrates that the method significantly improves the rejection of α pulses compared to the previously reported methods. With an FOM value of 1.25, almost complete rejection of the α pulses can be achieved. This method is especially useful for low-background measurements of high-energy γ rays in the environmental monitoring and security applications with large-size $LaBr_3$:(Ce) detectors, where the α background is a major problem. The method is also applicable to other types of scintillators where the difference in the shape of the pulses lies in the leading-edge of the pulses.

## Declaration of Competing Interest

The authors declare that they have no known competing financial interests or personal relationships that could have appeared to influence the work reported in this paper.

## Acknowledgement

The authors extend their appreciation to the deputyship for Research & Innovation, Ministry of Education in Saudi Arabia for funding this research work through the project number (IFP-2020-67).

## References

Alharbi, T. et al., 2015. Lifetime of the yrast $^1\pi$ = $^5-$ state and E1 hindrance in the transitional nucleus $^{13}_{65}$8Ce. Phys. Rev. C 91, 027302.
Alharbi, T., 2020. Pulse-shape discrimination of internal α-contamination in $LaBr_3$:(Ce) detectors by using the principal component analysis. J. Instrum. 15(06), P06010.
Bizarri, G., de Haas, J.T.M., Dorenbos, P., van Eijk, C.W.E., 2006. First time measurement of gamma-ray excited LaBr 3: 5% $C^{e3}$+ and $LaC_l$3: 10% $C^{e3}$+ temperature dependent properties. Phys. Status Solidi Appl. Res. 203 (5), R41–R43.
Crespi, F.C.L., Camera, F., Blasi, N., Bracco, A., Brambilla, S., Million, B., Nicolini, R., Pellegri, L., Riboldi, S., Sassi, M., Wieland, O., Quarati, F., Owens, A., 2009. Alpha–gamma discrimination by pulse shape in LaBr 3:(Ce) and $LaC_l$3:(Ce). Nucl. Instrum. Methods A 602 (2), 520–524.
Cang, J. et al., 2018. Mechanism of Pulse shape discrimination in LaBr 3:(Ce): Modeling with dynamic equations. IEEE Nucl. Sci. Symp. Med. Imag. Conf. Rec., 1
Cang, J., Fang, X., Zeng, Z., Zeng, M., Liu, Y., Sun, Z., Chen, Z., 2020. Ionization-density-dependent scintillation pulse shape and mechanism of luminescence quenching in LaBr 3:(Ce). Phys. Rev. Appl. 14 (6), 064075.
Dorenbos, P., Haas, J.D., van Eijk, C., 2004. Gamma ray spectroscopy with a 19 × 19 $mm^3$ LaBr 3: 0.5% $C^{e3}$+ scintillator. IEEE Trans. Nucl. Sci. 51, 1289–1296.
Hoel, C., Sobotka, L.G., Shah, K.S., Glodo, J., 2005. Pulse-shape discrimination of La halide scintillators. Nucl. Instrum. Methods A 540 (1), 205–208.
Lintereur, A. et al., 2002. Neutron and Gamma Ray Pulse Shape Discrimination with Polyvinyltoluene. Pacific Northwest Laboratory Report PNNL-21609.
McFee, J.E., Mosquera, C.M., Faust, A.A., 2016. Comparison of model fitting and gated integration for pulse shape discrimination and spectral estimation of digitized lanthanum halide scintillator pulses. Nucl. Instrum. Methods A 828, 105–115.
Moszyński, M., Nassalski, A., Syntfeld-Każuch, A., Szczęśniak, T., Czarnacki, W., Wolski, D., Pausch, G., Stein, J., 2006. Temperature dependences of LaBr 3(Ce), $LaC_l$3(Ce) and NaI (Tl) scintillators. Nucl. Instrum. Methods Phys. Res. A 568 (2), 739–751.
Milbrath, B.D., Runkle, R.C., Hossbach, T.W., Kaye, W.R., Lepel, E.A., McDonald, B.S., Smith, L.E., 2005. Characterization of alpha contamination in lanthanum trichloride scintillators using coincidence measurements. Nucl. Instrum. Methods Phys. Res. A 547 (2-3), 504–510.
Nicolini, R. et al., 2007. Investigation of the properties of a $\hat{\hat{1}}\times\hat{\hat{1}}$ LaBr 3:(Ce) scintillator. Nucl. Instrum. Methods A 582, 554–561.
Ogawara, R., Ishikawa, M., 2015. Feasibility study on signal separation for spontaneous alpha decay in LaBr 3:(Ce) scintillator by signal peak-to-charge discrimination. Rev. Sci. Instrum. 86 (8), 085108.
Singh, H., Mehra, R., 2017. Discrete wavelet transform method for high flux n−γ discrimination with liquid scintillators. IEEE Trans. Nucl. Sci. 64 (7), 1927.
Tang, Y.Y., 2014. Wavelet Theory Approach to Pattern Recognition. World Scientific, Singapore.
van Loef, E.V.D., Dorenbos, P., van Eijk, C.W.E., Krämer, K., Güdel, H.U., 2001. High-energy-resolution scintillator: $Ce^{3+}$ activated LaBr 3. Appl. Phys. Lett. 79 (10), 1573–1575.
van Loef, E.V.D., Dorenbos, P., van Eijk, C.W.E., Krämer, K.W., Güdel, H.U., 2002. Scintillation properties of LaBr 3:$(Ce^{)3}$+ crystals: Fast, efficient and high-energy-resolution scintillators. Nucl. Instrum. Methods A 486 (1-2), 254–258.
Vedia, V., Carmona-Gallardo, M., Fraile, L.M., Mach, H., Udías, J.M., 2017. Performance evaluation of novel LaBr 3(Ce) scintillator geometries for fast-timing applications. Nucl. Instrum. Methods A 857, 98–105.
Winyard, R.A., Lutkin, J.E., McBeth, G.W., 1971. Pulse shape discrimination in inorganic and organic scintillators. Nucl. Instrum. Meth. 95, 141–153.
Wolszczak, W., Dorenbos, P., 2017. Shape of intrinsic alpha pulse height spectra in lanthanide halide scintillators. Nucl. Instrum. Methods A 857, 66–74.
Yousefi, S., Lucchese, L., Aspinall, M.D., 2009. Digital discrimination of neutrons and gamma-rays in liquid scintillators using wavelets. Nucl. Instrum. Methods A 598 (2), 551–555.
Zeng, M., Cang, J., Zeng, Z., Yue, X., Cheng, J., Liu, Y., Ma, H., Li, J., 2016. Quantitative analysis and efficiency study of PSD methods for a LaBr 3:(Ce) detector. Nucl. Instrum. Methods A 813, 56–61.